AN OVERVIEW AND COMPARISON OF OTM FORMULATIONS ON THE BASIS OF THE MODE DISPLACEMENT METHOD AND THE MODE ACCELERATION METHOD

S.H.J.A. Fransen[1]
ESA/ESTEC - Structures Section TOS-MCS
PO Box 299
2200 AG Noordwijk
The Netherlands
bfransen@ymd.estec.esa.nl

Paper: 2001-17

ABSTRACT

An important step in the design and verification process of spacecraft structures is the coupled transient analysis with the launch vehicle in the low-frequency domain. In order to reduce the costs of computation, the spacecraft and launcher models have to be dynamically reduced before they are coupled together. Once the coupled analysis has been completed, the transient solution for the reduced spacecraft model is available. The recovery of physical displacements from this transient solution can be improved using *OTM*'s (*OTM* = Output Transformation Matrix) defined on the basis of the mode acceleration method instead of the mode displacement method. This also holds true for displacement-related data such as element forces, element stresses and multi point constraint forces. The aim of this paper is to give an overview of the *OTM* formulations, which are of practical use in space projects. The *OTM*'s will be derived according to both the mode displacement method and the mode acceleration method. The gain in accuracy when adopting the mode acceleration method will be demonstrated by means of a simple clamped beam example. The procedure to calculate the *OTM*'s has been programmed using MSC.Nastran *DMAP*. The *DMAP* alter has been used successfully by *ESA* in the frame of the International Space Station project, where coupled loads analysis with the space shuttle were required. Equipment racks have been reduced to *CB*-models and associated *OTM*'s have been generated.

[1] Consultant – Atos-Origin Engineering Services B.V.

NOMENCLATURE

Symbols & Acronyms

q	generalised coordinate (*DOF*)
t	time
x	displacement coordinate (*DOF*)
CB	Craig-Bampton
COG	center of gravity
D	stress-displacement relationship
DMAP	direct matrix abstraction program
DOF	degree of freedom
DTM	displacement transformation matrix
E	total number of elements
ESA	European Space Agency
F	interface force, constraint force component
FE	finite element
G	set transformation matrix
I	identity matrix, total number of internal *DOF*'s
ISS	International Space Station
J	identity matrix, total number of internal *DOF*'s
$K, \overline{K}$	stiffness matrix
LTM	interface force transformation matrix
$M, \overline{M}$	mass matrix
MAM	mode acceleration method
MDM	mode displacement method
MPC	multi point constraint
N	total number of physical *DOF*'s
NTM	*COG* net load factor transformation matrix
OTM	output transformation matrix
P	total number of normal modes
QTM	*MPC*-force transformation matrix
STM	element stress/force transformation matrix
f	constraint modes
j	normal modes with clamped interface
y	Craig-Bampton transformation matrix

Subscripts

e	element items
i	internal *DOF*'s
j	interface *DOF*'s
g	g-set *DOF*'s
m	m-set *DOF*'s associated with *MPC*'s
n	n-set *DOF*'s
p	generalised *DOF*'s
r	r-set interface *DOF*'s
rel	relative

Superscripts

T	transpose
-1	inverse

1. INTRODUCTION

In this paper *OTM*'s will be derived on the basis of both the mode displacement and the mode acceleration method. It will be shown that the mode acceleration method is the preferred method when physical data are recovered from a low frequency transient analysis with a dynamically reduced finite element model. The mode acceleration method improves the accuracy of the recovered physical displacements compared to the mode displacement method. As a consequence the differential of the displacements will be more accurate as well, which explains the gain in the accuracy of the element forces and stresses.

OTM's will be derived to enable the recovery of displacements, element forces, element stresses and *MPC* forces. The dynamic reduction technique practiced in this paper will be according to Craig and Bampton[1]. As a consequence the *OTM*'s derived, will be based on a reduced solution according to the Craig-Bampton method.

To complete the overview of *OTM*'s, the *OTM's* for the recovery of the interface forces and *COG* net load factors will be derived as well. The *OTM*'s for the recovery of the interface forces can be directly derived from the Craig-Bampton equations of motion. The accuracy of the interface forces cannot be improved by adopting a mode acceleration approach. Since the *OTM*'s for the recovery of the *COG* net load factors are derived from the *OTM*'s for the recovery of the interface forces, this also applies to them. This means both the *OTM's* for the recovery of the interface forces and *COG* net load factors belong to a different class of *OTM*'s of which the accuracy can only be improved by taking into account a higher number of modes.

The order of the sections is as follows. In section 2 the Craig-Bampton method is briefly discussed. In section 3 the *OTM*'s for the recovery of displacements, element forces, element stresses and MPC forces are derived on basis of the mode displacement method. In section 4 a similar set of *OTM*'s will be derived on basis of the mode acceleration method. Finally the *OTM*'s for the recovery of interface forces and *COG* net load factors are derived in section 5. In section 6 a description of the *DMAP* is given which incorporates the equations derived in sections 2 up to 5. In section 7 the *DMAP* is applied to a simple clamped beam in order to compute the *CB*-model and *OTM*'s on basis of the mode displacement and mode acceleration method. Furthermore a transient analysis is run to compare the

recovered solutions on basis of both methods. Section 8 is devoted to a reduction problem associated with the ISS project at ESA-ESTEC. In section 9 conclusions are formulated.

2. CRAIG-BAMPTON REDUCTION

Consider a free-free physical *FE*-model having *J* interface *DOF*'s and *I* internal *DOF*'s, which is only loaded at its interface. The equations of motion can then be written as follows in partitioned format, if damping is not considered:

$$\begin{bmatrix} M_{jj} & M_{ji} \\ M_{ij} & M_{ii} \end{bmatrix} \cdot \begin{pmatrix} \ddot{x}_j \\ \ddot{x}_i \end{pmatrix} + \begin{bmatrix} K_{jj} & K_{ji} \\ K_{ij} & K_{ii} \end{bmatrix} \cdot \begin{pmatrix} x_j \\ x_i \end{pmatrix} = \begin{pmatrix} F_j \\ 0 \end{pmatrix} \quad (1)$$

One can reduce the model dynamically by using a set of *P* normal modes and *J* constraint modes to describe the physical displacements. It should be noted that a considerable reduction of *DOF*'s can only be achieved in case $P<<I$. The transformation according to Craig and Bampton[1] is given by:

$$\begin{pmatrix} x_j \\ x_i \end{pmatrix} = y \cdot \begin{pmatrix} x_j \\ q_p \end{pmatrix} \quad (2)$$

where,

$$y = \begin{bmatrix} I_{jj} & 0_{jp} \\ f_{ij} & j_{ip} \end{bmatrix} \quad (3)$$

where f_{ij} are the constraint modes due to unit displacements of the interface *DOF*'s and j_{ip} are the normal modes with a fully constrained interface. The constraint modes are calculated fom the following static equilibrium equation:

$$K_{ij} \cdot I_{jj} + K_{ii} \cdot f_{ij} = 0 \quad (4)$$

or,

$$f_{ij} = -K_{ii}^{-1} \cdot K_{ij} \quad (5)$$

The normal modes are calculated from the following eigenvalue problem:

$$\begin{aligned} x_i &= j_i \cdot e^{iwt} \\ (w^2 \cdot M_{ii} - K_{ii}) \cdot j_i &= 0 \end{aligned} \quad (6)$$

The solution of this eigenvalue problem has *I* eigenvalues w^2 and a set of *I* eigenvectors j_{ii}. As such j_{ip} is a subset of the total modal basis of eigenvectors j_{ii}.

Substitution of eq.(2) into eq.(1) and pre-multiplication of eq.(1) with the transpose of the transformation matrix *y* gives the following reduced set of equations of motion:

$$\begin{bmatrix} \overline{M}_{jj} & M_{jp} \\ M_{pj} & M_{pp} \end{bmatrix} \cdot \begin{pmatrix} \ddot{x}_j \\ \ddot{q}_p \end{pmatrix} + \begin{bmatrix} \overline{K}_{jj} & 0 \\ 0 & K_{pp} \end{bmatrix} \cdot \begin{pmatrix} x_j \\ q_p \end{pmatrix} = y^T \cdot \begin{pmatrix} F_j \\ 0 \end{pmatrix} = \begin{pmatrix} F_j \\ 0 \end{pmatrix} \quad (7)$$

Solving this set of equations gives the solution in terms of interface *DOF*'s and generalised *DOF*'s. Substitution of the *CB*-solution into eq.(2) yields the physical solution according to the so-called mode displacement method.

For the matrices in eq.(7) the following relations hold:

$$\overline{M}_{jj} = M_{jj} + M_{ji} \cdot f_{ij} + f_{ij}^T \cdot M_{ij} + f_{ij}^T \cdot M_{ii} \cdot f_{ij} \quad (8)$$

$$M_{jp} = M_{ji} \cdot j_{ip} + f_{ij}^T \cdot M_{ii} \cdot j_{ip} \quad (9)$$

Assuming mass normalised modes:

$$M_{pp} = I_{pp} \quad (10)$$

$$\overline{K}_{jj} = K_{jj} + K_{ji} \cdot f_{ij} \quad (11)$$

$$K_{pp} = diag(w_p^2) \quad (12)$$

3. MODE DISPLACEMENT METHOD

In this section the *OTM*'s will be derived for the recovery of displacements, element forces and stresses and *MPC* forces on the basis of the mode displacement method. Since the static contribution of the truncated high frequency modes (*I-P* modes) is missing, all *OTM*'s derived in this section will lead to less accurate physical results than those obtained by *OTM*'s on the basis of the mode acceleration method. The latter will be derived in section 4.

3.1 RECOVERY OF DISPLACEMENTS

The recovery of physical displacements according to the mode displacement method is simply done by eq.(2), which can also be written as:

$$\begin{pmatrix} x_j \\ x_i \end{pmatrix} = DTM \cdot \begin{pmatrix} x_j \\ q_p \end{pmatrix} \quad (13)$$

where,

$$DTM = y \quad (14)$$

In this way the Craig-Bampton displacement set will be expanded to the physical displacement set.

3.2 RECOVERY OF ELEMENT STRESSES

Suppose the number of element stresses to be resolved, equals *E*. Then the element stresses can be calculated from:

$$s_e = \begin{bmatrix} D_{ej} & D_{ei} \end{bmatrix} \cdot \begin{pmatrix} x_j \\ x_i \end{pmatrix} \tag{15}$$

The matrix *D* is a differential operator calculating element strains from the node displacements. It also multiplies the strains with material properties according to the stress-strain relationship to obtain stresses. A similar relation also holds for element forces. Hence no distinction will be made between stresses and forces.

Substituting eq.(2) into eq.(15) one can derive:

$$s_e = STM \cdot \begin{pmatrix} x_j \\ q_p \end{pmatrix} \tag{16}$$

Using eq.(3) for the transformation matrix *y* one can derive for the *STM*:

$$STM = \begin{bmatrix} D_{ej} & D_{ei} \end{bmatrix} \cdot \begin{bmatrix} I_{jj} & 0_{jp} \\ f_{ij} & j_{ip} \end{bmatrix} \tag{17}$$

or,

$$STM = \begin{bmatrix} D_{ej} + D_{ei} \cdot f_{ij} & D_{ei} \cdot j_{ip} \end{bmatrix} \tag{18}$$

The recovery of element forces and stresses on the basis of the mode displacement method can now be conducted by means of eq.(16) and (18). Considering the *y* matrix in eq.(17) as a set of displacement solutions of the physical FE-model, one can calculate the *STM* by means of the SDR2 module of MSC.Nastran.

3.3. RECOVERY OF MPC-FORCES

To explain the recovery of *MPC*-forces, a set of equations will be presented which describes the procedure for the incorporation of *MPC*'s in MSC.Nastran. Schaeffer[2] explains how the *MPC*'s are represented in MSC.Nastran for a static problem. Here the extension from statics to dynamics is made, also illustrated by Craig[3].

The equations of motion (1) can also be partitioned as follows, in case MPC-equations are defined in the physical model:

$$\begin{bmatrix} M_{mm} & M_{mn} \\ M_{nm} & M_{nn} \end{bmatrix} \cdot \begin{pmatrix} \ddot{x}_n \\ \ddot{x}_m \end{pmatrix} + \begin{bmatrix} K_{mm} & K_{mn} \\ K_{nm} & K_{nn} \end{bmatrix} \cdot \begin{pmatrix} x_m \\ x_n \end{pmatrix} = \begin{pmatrix} P_m \\ P_n \end{pmatrix} + \begin{pmatrix} F_m \\ F_n \end{pmatrix} \tag{19}$$

In eq.(19) the constraint forces at the dependent *m*-set and independent *n*-set *DOF*'s are respectively called F_m and F_n. The applied interface loads F_j are part of P_m and/or P_n.

Eq. (19) can also be written as:

$$\begin{bmatrix} M_{mg} \\ M_{ng} \end{bmatrix} \cdot \begin{pmatrix} \ddot{x}_m \\ \ddot{x}_n \end{pmatrix} + \begin{bmatrix} K_{mg} \\ K_{ng} \end{bmatrix} \cdot \begin{pmatrix} x_m \\ x_n \end{pmatrix} = \begin{pmatrix} P_m \\ P_n \end{pmatrix} + \begin{pmatrix} F_m \\ F_n \end{pmatrix} \tag{20}$$

or,

$$M_{gg} \cdot \ddot{x}_g + K_{gg} \cdot x_g = P_g + F_g \tag{21}$$

The dependent *m*-set DoFs are related to the independent *n*-set DoFs by the following *MPC*-equations:

$$x_m = G_{mn} \cdot x_n \tag{22}$$

Then the g-set displacements can be expressed in terms of n-set displacements as:

$$x_g = \begin{bmatrix} G_{mn} \\ I_{nn} \end{bmatrix} \cdot x_n \tag{23}$$

or,

$$x_g = G_{gn} \cdot x_n \tag{24}$$

The reduced set of equations of motion, to solve the *n*-set unknowns, is then found by noting that the constraint forces F_g perform no work during a virtual displacement x_g:

$$x_g^{\ T} \cdot (F_g) = 0 \mid \forall x_g \tag{25}$$

Substitution of F_g found from eq.(21) yields:

$$x_g^{\ T} \cdot (M_{gg} \cdot \ddot{x}_g + K_{gg} \cdot x_g - P_g) = 0 \mid \forall x_g \tag{26}$$

Substitution of eq.(24) into eq.(26) leads to the following reduced set of equations of motion for the independent *n*-set *DOF*'s:

$$\overline{M}_{nn} \cdot \ddot{x}_n + \overline{K}_{nn} \cdot x_n = \overline{F_n} \tag{27}$$

where,

$$\overline{M}_{nn} = G_{gn}{}^{T} \cdot M_{gg} \cdot G_{gn} \quad (28)$$

$$\overline{K}_{nn} = G_{gn}{}^{T} \cdot K_{gg} \cdot G_{gn} \quad (29)$$

$$\overline{F}_{n} = G_{gn}{}^{T} \cdot P_{g} \quad (30)$$

The *n*-set solution can now be obtained by solving eq.(27). Afterwards the *m*-set solution is obtained from eq.(22).

The *m*-set *MPC*-forces can be solved from the *m*-set equations of motion in eq.(20):

$$F_m = M_{mg} \cdot \begin{pmatrix} \ddot{x}_n \\ \ddot{x}_m \end{pmatrix} + K_{mg} \cdot \begin{pmatrix} x_n \\ x_m \end{pmatrix} - P_m \quad (31)$$

Now the *m*-set MPC forces are known, the *n*-set forces can be solved from eq.(25) splitting it up into the *m*-set and *n*-set:

$$x_n{}^{T} \cdot F_n + x_m{}^{T} \cdot F_m = 0 \,|\, \forall x_g \quad (32)$$

or after substitution of eq.(22),

$$x_n{}^{T} (F_n + G_{mn}{}^{T} \cdot F_m) = 0 \,|\, \forall x_n \quad (33)$$

Eq.(47) then gives the following equilibrium equation:

$$F_n = -G_{mn}{}^{T} \cdot F_m \quad (34)$$

This equation will result in non-zero F_n values for the *n*-set *DOF*'s associated with the *MPC*'s. Note it would be much more expensive to solve F_n from the *n*-set equations of motion in eq.(20). Equations (31) and (34) will now be used to define the *OTM*'s for the recovery of *MPC*-forces.

Substitution of the second derivative of eq.(2) and its second derivative into eq.(31) gives:

$$F_m = QTM_{1m} \cdot \begin{pmatrix} \ddot{x}_j \\ \ddot{q}_p \end{pmatrix} + QTM_{2m} \cdot \begin{pmatrix} x_j \\ q_p \end{pmatrix} - P_m \quad (35)$$

where,

$$QTM_{1m} = M_{mg} \cdot y \quad (36)$$

and,

$$QTM_{2m} = K_{mg} \cdot y \quad (37)$$

From eq.(34) and eq.(35) one can derive for the *n*-set *MPC*-forces:

$$F_n = QTM_{1n} \cdot \begin{pmatrix} \ddot{x}_j \\ \ddot{q}_p \end{pmatrix} + QTM_{2n} \cdot \begin{pmatrix} x_j \\ q_p \end{pmatrix} + G_{mn}{}^{T} \cdot P_m \quad (38)$$

where,

$$QTM_{1n} = -G_{mn}{}^{T} \cdot QTM_{1m} \quad (39)$$

and,

$$QTM_{2n} = -G_{mn}{}^{T} \cdot QTM_{2m} \quad (40)$$

Combination of equations (35) and (38) yields:

$$F_g = QTM_1 \cdot \begin{pmatrix} \ddot{x}_j \\ \ddot{q}_p \end{pmatrix} + QTM_2 \cdot \begin{pmatrix} x_j \\ q_p \end{pmatrix} + QTM_3 \cdot P_m \quad (41)$$

where,

$$QTM_1 = \begin{bmatrix} QTM_{1m} \\ QTM_{1n} \end{bmatrix} \quad (42)$$

$$QTM_2 = \begin{bmatrix} QTM_{2m} \\ QTM_{2n} \end{bmatrix} \quad (43)$$

$$QTM_3 = \begin{bmatrix} -I_{mm} \\ G_{mn}{}^{T} \end{bmatrix} \quad (44)$$

Since the *r*-set, associated with the interface *DOF*'s, and the *m*-set, associated with dependent *MPC-DOF*'s, are mutually exclusive in MSC.Nastran, P_m does not contain any interface loads. Hence QTM_3 equals zero and eq.(41) can be reduced to:

$$F_g = QTM_1 \cdot \begin{pmatrix} \ddot{x}_j \\ \ddot{q}_p \end{pmatrix} + QTM_2 \cdot \begin{pmatrix} x_j \\ q_p \end{pmatrix} \quad (45)$$

3.4 DAMPING CONSIDERATIONS

The derivation of the *DTM* and *STM* recovery matrices on the basis of the mode displacement method, would be identical for systems with damping, also when the damping forces are considerable compared to the inertia and stiffness forces. The reason for this observation is that those recovery matrices are based on the transformation matrix ? rather than on the equations of motion. If the derivation of the *OTM*'s is based on the equations of motion (1), which is true for *OTM*'s for the recovery of *MPC*-forces, then the effect of damping is not taken into account. However, the recovery of *MPC*-forces according to eq.(45) is still valid for systems which are lightly damped, like typical spacecraft structures. For highly damped structures, the damping

matrix should be included in the derivation of the *OTM*'s for the *MPC*-forces.

4. MODE ACCELERATION METHOD

In the previous section the *OTM*'s were derived for the recovery of physical data on the basis of the mode displacement method. The physical data to be recovered were the displacements themselves or data dependent of the displacements. The accuracy of this physical data can be improved by deriving the *OTM*'s on the basis of the mode acceleration method, as also explained by Klein, Reynolds and Ricks[4]. In the mode acceleration method the solution for the physical displacements is improved by incorporating the static contribution of the truncated high frequency modes, as explained in many books, refer for instance to Craig[3], Petyt[5] or Géradin and Rixen[6]. For this purpose the physical equations of motion (1) are taken as the starting point, and are split into two parts:

$$\begin{bmatrix} M_{jj} & M_{ji} \end{bmatrix} \cdot \begin{pmatrix} \ddot{x}_j \\ \ddot{x}_i \end{pmatrix} + \begin{bmatrix} K_{jj} & K_{ji} \end{bmatrix} \cdot \begin{pmatrix} x_j \\ x_i \end{pmatrix} = F_j \tag{46}$$

$$\begin{pmatrix} x_j \\ x_i \end{pmatrix} = \begin{bmatrix} 0 & 0 \\ -K_{ii}^{-1} \cdot M_{ij} & -K_{ii}^{-1} \cdot M_{ii} \end{bmatrix} \cdot \begin{pmatrix} \ddot{x}_j \\ \ddot{x}_i \end{pmatrix} + \begin{bmatrix} I \\ -K_{ii}^{-1} \cdot K_{ij} \end{bmatrix} \cdot x_j \tag{47}$$

Eq.(47) expresses the physical displacements as a function of the physical accelerations and interface displacements. This equation will now be used to improve the quality of the *OTM*'s needed for the recovery of displacements and related data from a Craig-Bampton solution.

4.1 RECOVERY OF DISPLACEMENTS

Substitution of the second derivative of eq.(2) into eq.(47) gives the complete set of physical displacements of which the internal displacements are corrected according to the mode acceleration method:

$$\begin{pmatrix} x_j \\ x_i \end{pmatrix} = \begin{bmatrix} 0 & 0 \\ -K_{ii}^{-1} \cdot M_{ij} & -K_{ii}^{-1} \cdot M_{ii} \end{bmatrix} \cdot y \cdot \begin{pmatrix} \ddot{x}_j \\ \ddot{q}_p \end{pmatrix} + \begin{bmatrix} I \\ -K_{ii}^{-1} \cdot K_{ij} \end{bmatrix} \cdot x_j \tag{48}$$

Substituting the transformation matrix (eq.(3)) into eq.(48), one can derive the following equation for the recovery of physical displacements according to the mode acceleration method:

$$\begin{pmatrix} x_j \\ x_i \end{pmatrix} = DTM_1 \cdot \begin{pmatrix} \ddot{x}_j \\ \ddot{q}_p \end{pmatrix} + DTM_2 \cdot x_j \tag{49}$$

where,

$$DTM_1 = \begin{bmatrix} 0 & 0 \\ -K_{ii}^{-1} \cdot M_{ij} & -K_{ii}^{-1} \cdot M_{ii} \end{bmatrix} \cdot \begin{bmatrix} I_{jj} & 0_{jp} \\ f_{ij} & j_{ip} \end{bmatrix} \tag{50}$$

or,

$$DTM_1 = \begin{bmatrix} 0 & 0 \\ -K_{ii}^{-1} \cdot (M_{ij} + M_{ii} f_{ij}) & -K_{ii}^{-1} \cdot M_{ii} \cdot j_{ip} \end{bmatrix} \tag{51}$$

and,

$$DTM_2 = \begin{bmatrix} I_{jj} \\ -K_{ii}^{-1} \cdot K_{ij} \end{bmatrix} \tag{52}$$

or (using eq.(5) for the constraint modes):

$$DTM_2 = \begin{bmatrix} I_{jj} \\ f_{ij} \end{bmatrix} \tag{53}$$

DTM_1 has a size of $(J+I)$x$(J+P)=N$x$(J+P)$ and DTM_2 has a size of $(J+I)$x$J=N$xJ.

4.2 RECOVERY OF STRESSES

Substitution of eq.(48) into eq.(15) one can derive:

$$s_e = STM_1 \cdot \begin{pmatrix} \ddot{x}_j \\ \ddot{q}_p \end{pmatrix} + STM_2 \cdot x_j \tag{54}$$

where,

$$STM_1 = \begin{bmatrix} D_{ej} & D_{ei} \end{bmatrix} \cdot \begin{bmatrix} 0 & 0 \\ -K_{ii}^{-1} \cdot M_{ij} & -K_{ii}^{-1} \cdot M_{ii} \end{bmatrix} \cdot \begin{bmatrix} I_{jj} & 0_{jp} \\ f_{ij} & j_{ip} \end{bmatrix} \tag{55}$$

or,

$$STM_1 = \begin{bmatrix} -D_{ei} \cdot (K_{ii}^{-1} \cdot M_{ij} + K_{ii}^{-1} \cdot M_{ii} \cdot f_{ij}) & -D_{ei} \cdot K_{ii}^{-1} \cdot M_{ii} \cdot j_{ip} \end{bmatrix} \tag{56}$$

and,

$$STM_2 = \begin{bmatrix} D_{ej} & D_{ei} \end{bmatrix} \cdot \begin{bmatrix} I_{jj} \\ -K_{ii}^{-1} \cdot K_{ij} \end{bmatrix} \tag{57}$$

or (using eq.(5) for the constraint modes),

$$STM_2 = D_{ej} + D_{ei} \cdot f_{ij} \tag{58}$$

STM_1 has a size of Ex$(J+P)$ and STM_2 has a size of ExJ. Note that $LTM_2=0$ for a statically determinate structure, which by definition causes no stresses due to interface deformation.

4.3 RECOVERY OF MPC-FORCES

Substitution of the second derivative of eq.(2) and eq.(49) into eq.(31) gives:

$$F_m = QTM_{1m} \cdot \begin{pmatrix} \ddot{x}_j \\ \ddot{q}_p \end{pmatrix} + QTM_{2m} \cdot x_j - P_m \tag{59}$$

where,

$$QTM_{1m} = M_{mg} \cdot y + K_{mg} \cdot DTM_1 \tag{60}$$

and,

$$QTM_{2m} = K_{mg} \cdot DTM_2 \tag{61}$$

From eq.(34) and eq.(59) one can derive for the *n*-set *MPC*-forces:

$$F_n = QTM_{1n} \cdot \begin{pmatrix} \ddot{x}_j \\ \ddot{q}_p \end{pmatrix} + QTM_{2n} \cdot x_j + G_{mn}{}^T \cdot P_m \tag{62}$$

where,

$$QTM_{1n} = -G_{mn}{}^T \cdot QTM_{1m} \tag{63}$$

and,

$$QTM_{2n} = -G_{mn}{}^T \cdot QTM_{2m} \tag{64}$$

Combination of eqs.(59) and (62) gives:

$$\begin{pmatrix} F_m \\ F_n \end{pmatrix} = \begin{bmatrix} QTM_{1m} \\ QTM_{1n} \end{bmatrix} \cdot \begin{pmatrix} \ddot{x}_j \\ \ddot{q}_p \end{pmatrix} + \begin{bmatrix} QTM_{2m} \\ QTM_{2n} \end{bmatrix} \cdot x_j + \begin{bmatrix} -I_{mm} \\ G_{mn}{}^T \end{bmatrix} \cdot P_m \tag{65}$$

or,

$$F_g = QTM_1 \cdot \begin{pmatrix} \ddot{x}_j \\ \ddot{q}_p \end{pmatrix} + QTM_2 \cdot x_j + QTM_3 \cdot P_m \tag{66}$$

where,

$$QTM_1 = \begin{bmatrix} QTM_{1m} \\ QTM_{1n} \end{bmatrix} \tag{67}$$

$$QTM_2 = \begin{bmatrix} QTM_{2m} \\ QTM_{2n} \end{bmatrix} \tag{68}$$

$$QTM_3 = \begin{bmatrix} -I_{mm} \\ G_{mn}{}^T \end{bmatrix} \tag{69}$$

As explained in section 3.3, P_m does not contain any interface loads. For that reason QTM_3 equals zero and eq.(66) reduces to:

$$F_g = QTM_1 \cdot \begin{pmatrix} \ddot{x}_j \\ \ddot{q}_p \end{pmatrix} + QTM_2 \cdot x_j \tag{70}$$

For a structure with a statically determinate interface, the *MPC*-forces should be zero for arbitrary interface displacements. Therefore QTM_2 equals zero in case of a statically determinate interface.

4.4 DAMPING CONSIDERATIONS

As already stated in section 3.4, the effect of damping is not taken into account in the derivation of the *OTM*'s, if they are based on the equations of motion (1). This is true for all *OTM*'s based on the mode acceleration approach as derived in sections 4.1, 4.2 and 4.3. However, the recovery equations (49), (54) and (70) are still valid for lightly damped systems, like typical spacecraft structures. For highly damped systems the equations of motions with damping included should be taken as the starting point to derive the *OTM*'s.

5. RECOVERY OF INTERFACE FORCES AND COG NET LOAD FACTORS

As stated in the introduction another class of *OTM*'s exists which cannot be improved by using the mode acceleration method. Those are the *OTM*'s for the recovery of the interface forces and the related *OTM*'s for the recovery of the *COG* net load factors.

5.1 RECOVERY OF INTERFACE FORCES

Splitting the *CB* equations of motion (7) into an interface part (upper set) and modal part (lower set), the following equations can be derived:

$$\begin{bmatrix} \overline{M}_{jj} & M_{jp} \end{bmatrix} \cdot \begin{pmatrix} \ddot{x}_j \\ \ddot{q}_p \end{pmatrix} + \overline{K}_{jj} \cdot x_j = F_j \tag{71}$$

$$\begin{pmatrix} x_j \\ q_p \end{pmatrix} = \begin{bmatrix} 0 & 0 \\ -K_{pp}{}^{-1} \cdot M_{pj} & -K_{pp}{}^{-1} \cdot M_{pp} \end{bmatrix} \cdot \begin{pmatrix} \ddot{x}_j \\ \ddot{q}_p \end{pmatrix} + \begin{bmatrix} I_{jj} \\ 0 \end{bmatrix} \cdot x_j \tag{72}$$

If the Craig-Bampton model is part of a bigger system of models, then the interface forces can be calculated from eq.(71). Equation (72) expresses the *CB*-space displacements in terms of the *CB*-space accelerations and the physical interface displacements. Pre-multiplication of the upper part of eq.(1) with the transpose of the transformation matrix y and subsequent substitution of the expanded Craig-Bampton solution into eq.(1) would lead directly to eq.(71). Hence there is no difference in accuracy between recovery with eq.(71) or recovery by substitution of the expanded *CB* accelerations and displacements in eq.(1). A mode acceleration expression is not possible in this case. Hence, the

only way to increase the accuracy is to include more modes. The *OTM*'s for the recovery of interface forces can therefore be classified as a separate class.

Equation (71) can also be written as:

$$F_j = LTM_1 \cdot \begin{pmatrix} \ddot{x}_j \\ \ddot{q}_p \end{pmatrix} + LTM_2 \cdot x_j \tag{73}$$

where,

$$LTM_1 = \begin{bmatrix} \overline{M}_{jj} & M_{jp} \end{bmatrix} \tag{74}$$

$$LTM_2 = \overline{K}_{jj} \tag{75}$$

For a statically determinate interface it is known that the interface forces and internal forces are zero for any arbitrary displacement x_j:

$$\begin{bmatrix} K_{jj} & K_{ji} \\ K_{ij} & K_{ii} \end{bmatrix} \cdot \begin{pmatrix} x_j \\ x_i \end{pmatrix} = \begin{pmatrix} 0 \\ 0 \end{pmatrix} | \forall x_j \tag{76}$$

The second row gives:

$$x_i = -K_{ii}^{-1} \cdot K_{ij} \cdot x_j = f_{ij} \cdot x_j \tag{77}$$

Substitution of eq.(77) into the first row of eq.(76) gives:

$$(K_{jj} + K_{ji} \cdot f_{ij}) \cdot x_j = 0 | \forall x_j \tag{78}$$

Comparing the equations (78) and (11), one can see that $\overline{K}_{jj}$=0 for a statically determinate interface. As such one can conclude from eq.(75) that for this special case LTM_2=0.

5.2 RECOVERY OF COG NET LOAD FACTORS

The *COG* net load factors are defined as the accelerations in the component COG due to the recovered interface forces as if it were a rigid structure. Consider a *FE*-model, which is loaded at its interface only. For each point in time, the equilibrium force at the *COG* is calculated as follows:

$$F_{COG} = f_{Rj}^{\ T} \cdot F_j \tag{79}$$

Here f_{Rj} are the 6 rigid body vectors relative to the *COG* associated with the interface *DOF*'s and F_{COG} is a force vector with 6 components. Now the *COG* net load factors can be calculated as:

$$a_{COG} = M_R^{-1} \cdot F_{COG} \tag{80}$$

where the rigid body mass matrix at the *COG* is given by:

$$M_R = f_R^{\ T} \cdot M \cdot f_R \tag{81}$$

Substitution of equation (80) into (79) yields:

$$a_{COG} = M_R^{-1} \cdot f_{Rj}^{\ T} \cdot F_j \tag{82}$$

Substitution of the interface forces F_j according to eq.(73) yields:

$$a_{COG} = NTM_1 \cdot \begin{pmatrix} \ddot{x}_j \\ \ddot{q}_p \end{pmatrix} + NTM_2 \cdot x_j \tag{83}$$

where NTM_1 is given by,

$$NTM_1 = M_R^{-1} \cdot f_{Rj}^{\ T} \cdot LTM_1 \tag{84}$$

and NTM_2 is given by,

$$NTM_2 = M_R^{-1} \cdot f_{Rj}^{\ T} \cdot LTM_2 \tag{85}$$

5.3 DAMPING CONSIDERATIONS

Since the derivation of the *OTM*'s for the recovery of interface forces and *COG* net load factors is based on the equations of motion (1), the recovery equations (73), and (83) are only valid for systems which are lightly damped, like typical spacecraft structures. For highly damped systems the equations of motions with damping included should be taken as the starting point to derive the *OTM*'s.

6. DMAP

Tong and Chang[7] developed a *DMAP* alter for MSC.Nastran SOL 103, version 67, to generate *CB*-models and *OTM*'s for the recovery of accelerations, interface forces, displacements and element forces. This *DMAP* was used as a baseline for implementing all functionality described in the previous sections. Compared to Tong and Chang[7] the following functionality was added:

- *OTM*'s for element stresses
- *OTM*'s for *MPC* forces
- *OTM*'s for *COG* net load factors
- Tools to reduce the *OTM*'s to the required *DOF*'s
- Incorporation of the single point constraint *s*-set *DOF*'s and *MPC* related dependent *m*-set *DOF*'s in the matrices y, DTM_1 and DTM_2.

The *DMAP* alter runs with MSC.Nastran SOL 103, version 70.5. The complete functionality of the *DMAP* alter can be summarised as follows:

- generates *CB* mass and stiffness matrix

- generates the transformation matrix y
- generates the recovery matrices LTM_1 and LTM_2 for the recovery of interface forces
- generates the recovery matrix *DTM* (mode displacement method) or the matrices DTM_1 and DTM_2 (mode acceleration method) for the recovery of displacements for a specified set of *DOF*'s
- generates the recovery matrix *STM* (mode displacement method) or the matrices STM_1 and STM_2 (mode acceleration method) for the recovery of element stresses for a specified set of elements
- generates a similar *OTM*'s as noted under the previous point for the recovery of element forces
- Generates the recovery matrix *QTM* (mode displacement method) or the matrices QTM_1 and QTM_2 for the recovery of constraint forces resulting from *MPC*'s

The user has to define some parameters in the bulk data deck to control the *DMAP*.

7. TEST PROBLEM

In order to test the DMAP a test model was prepared. A transient analysis was run with the physical model and CB-model, in order to compare the solutions.

7.1 PROBLEM DEFINITION

A simple beam model with a statically indeterminate interface was defined to test the *DMAP*. Refer to figure 1 where the physical model is shown. The beam consists of mainly bar elements (CBAR) and one rigid body element (RBE2). The total span of the beam is 100 meters. Furthermore a rigid body support is defined such that the end nodes of the beam are rigidly connected. Stiff springs (CELAS2 elements) are defined between the rigid support and the beam, i.e. between nodes 100&300 and nodes 110&310. In the true model those node couples are coincident. The rigid support is meant to accelerate the end nodes of the beam, nodes 100 and 110, simultaneously in the course of a transient analysis. To conduct the transient analysis the big mass method is used, with a big mass at node 320.

The part of the beam model, which includes nodes 100 through 110, has 60 independent *DOF*'s and weighs 45 kg. This part of the physical model will be subject to Craig-Bampton reduction, as shown in figure 1. The *CB*-model has the following characteristics:

- 12 physical interface *DOF*'s of nodes 100 and 110
- 2 generalised *DOF*'s

The 2 modes associated with the generalised *DOF*'s have a total effective mass equal to 80% of the rigid mass and can be identified as the first bending modes in the x-y plane and the x-z plane.

After having created the *CB*-model and all *OTM*'s, the *CB*-model (+ rigid support) and physical model were subjected to a transient analysis for comparison. A modal viscous damping factor of 2.5% applies to both transient analyses. Both models are loaded at node 320 with a linear increasing acceleration in z-direction until t=0.8 s, where it reaches an acceleration of 1 m/s^2. This acceleration is kept constant for the rest of the run-time, i.e. until t=10 s. For t>0.8 seconds the model will lift-off in z-direction with a linearly increasing velocity. The displacement increases with the square of time.

Subsequently the *CB*-solution was used together with the *OTM*'s to recover the physical solution. Where applicable, results were recovered both according to the mode displacement method and the mode acceleration method. The recovered physical solution in terms of interface forces, accelerations, displacements, element stresses and forces and *MPC*-forces was compared with the solution obtained from the transient analysis of the physical model (no modal truncation). In section 7.2 only the results for the displacements and stresses will be highlighted for reasons of brevity.

7.2 ANALYSES RESULTS

In figure 2 the input acceleration at node 100 is compared with the *CB* recovered acceleration at node 100. Both are equal according to expectation. From figure 3 up to figure 6 the recovered solutions according to the mode acceleration method (*MAM*) and the mode displacement method (*MDM*) are compared with the physical solution. Plotting the relative displacements (i.e. relative to the rigid body movement), one can observe the difference in accuracy between the mode displacement and mode acceleration method, refer to figures 3 and 4. The relative displacements according to the mode acceleration method were obtained using total accelerations and relative displacements as follows:

$$\begin{pmatrix} x_j \\ x_i \end{pmatrix}_{rel} = DTM_1 \cdot \begin{pmatrix} \ddot{x}_j \\ \ddot{q}_p \end{pmatrix} + DTM_2 \cdot \left(x_j\right)_{rel} \qquad (86)$$

Obviously the mode displacement method fails in accuracy in case low-frequency or constant loads are applied to the CB-model. Part of the static behaviour is missing due to modal truncation. Even more drastic differences can be observed for displacement-related

data such as the element stresses. The reason for this observation is that these quantities are related to the differential of the relative displacements, giving even greater errors. It should be noted that all quantities should converge to the values found for a static analysis with a gravity field of 1 m/s^2 (see figure 2). For the mode displacement method this convergence value has an offset, which can be regarded as the error due to modal truncation. For the element stress as plotted in figure 5 and 6, the error for the mode displacement method and the mode acceleration method relative to the physical solution is plotted in figure 7. The error for the mode displacement method is greater than 10^{-2} whereas the mode acceleration method shows an error of 10^{-3} and less.

8. ISS EQUIPMENT RACK

For a transient coupled loads analysis with the space shuttle, a CB-model had to be generated of a payload rack as shown in figure 8. In order to recover the physical data from the CB-space transient solution, *OTM*'s were requested as well. The *CB*-reduction and *OTM* generation was performed according to Nieder [8]. Payload racks are usually part of habitable modules, like *ESA*'s Columbus Orbital Facility (*COF*) depicted in figure 9. The rack considered here, is part of a similar module used for transportation of pressurised payloads.

The payload rack, having about 200000 *DOF*'s, was reduced to a *CB*-model with 30 interface *DOF*'s and 200 generalised *DOF*'s. The sum of the effective mass of the 200 retained normal modes was greater than 90% of the rigid mass of the rack. The properties of the matrices delivered to the coupled loads analysis authority are given in table 1.

matrix	type	method	size
MCB	*CB*-system	*CB*	230 x 230
KCB	*CB*-system	*CB*	230 x 230
ATM[A)]	*OTM*	-	848 x 230
LTM_1	*OTM*	-	14 x 230
LTM_2	*OTM*	-	14 x 30
DTM_1	*OTM*	*MAM*	1887 x 230
DTM_2	*OTM*	*MAM*	1887 x 30
STM_1	*OTM*	*MAM*	4548 x 230
STM_2	*OTM*	*MAM*	4548 x 30
STM_1[B)]	*OTM*	*MAM*	135 x 230
STM_2	*OTM*	*MAM*	135 x 30
QTM_1	*OTM*	*MAM*	1069 x 230
QTM_2	*OTM*	*MAM*	1069 x 30

[A)] Acceleration transformation matrix = row partition of y
[B)] Second set of *STM*'s for recovery of element forces

Table 1: *CB* and *OTM* matrices

Each *OTM* listed in table 1 was checked by comparing the transient output of a recovery item of the physical model and of the *CB*-model. The same approach was used in the test problem of section 7.

9. CONCLUSIONS

A *DMAP* alter has been developed to create component Craig-Bampton models. The *DMAP* alter generates the *CB* mass and stiffness matrix and recovery matrices for accelerations, interface forces, *COG* net load factors, displacements, element forces, element stresses and *MPC*-forces. The latter four items can be defined according to the mode displacement method or mode acceleration method, which uses the full physical mass and stiffness matrix to incorporate the static contribution of the truncated modes. This will be advantageous if low frequency (compared to cut-off frequency) forcing functions are defined to excite the structure. The solution for the physical displacements will be more accurate. The accuracy of the element stresses and forces will improve, since they are dependent of the differential of the recovered displacements (strain). The accuracy of the *MPC*-forces will improve for the same reason. However, the *MPC*-forces are also dependent of the inertia forces.

Of course the mode acceleration method also has a disadvantage. In case of a high damping ratio, the mode displacement method (except for the *MPC*-force recovery according to the mode displacement method) will be more accurate, since damping has been neglected in the formulation of the mode acceleration method. Fortunately high damping values are not very common for spacecraft structures.

ACKNOWLEDGEMENTS

The author would like to thank the following persons for their comments and suggestions: D. Rixen, TU-Delft, A. Renwick, Atos-Origin, M. Klein, ESA-ESTEC, R. Bureo Dacal, ESA-ESTEC, T. Henriksen, ESA-ESTEC.

REFERENCES:

[1] Craig, R.R., Jr., and Bampton, M.C.C., *"Coupling of Substructures for Dynamic Analysis,"* AIAA Journal, Vol. 6, No. 7, 1968, pp. 1313-1319.

[2] Schaeffer, H.G., *MSC/NASTRAN Primer – Static and Normal Modes Analysis,"* Wallace Press, Inc., Milford, New Hampshire, 1988.

[3] Craig, , R.R., Jr., "*Structural Dynamics – An intoduction to computer methods,*" John Wiley & Sons, Inc., New York, NY, 1981.

[4] Klein, M., Reynolds, J., and Ricks, E., "*Derivation of improved Load Transformation Matrices for Launchers-Spacecraft coupled Analysis, and direct Computation of Margins of Safety,*" Proc. International Conference: "Spacecraft Structures and Mechanical Testing", 1989.

[5] Petyt, M., "*Introduction to Finite Element Vibration Analysis,*" Cambridge University Press, New York, NY, 1990.

[6] Géradin, M., and Rixen, D., "*Mechanical Vibrations – Theory and Application to Structural Dynamics,*" John Wiley & Sons, Ltd., Chichester, England, 1997.

[7] Tong, E.T., and Chang, C.C.J., "*An efficient Procedure for Data Recovery of a Craig-Bampton Component,*" MSC Nastran World User's Conference, Orlando, Florida, 1994.

[8] Nieder, R.L., "*Structural Integration Analyses Responsibility Definition for Space Shuttle Vehicle and Cargo Element Developers,*" NSTS 37329, Lyndon B. Johnson Space Center, Houston, Texas, 2000.

[9] Fransen, S.H.J.A., *"MSG Rack – OTM and CB-Model Description,"* TOS-MCS/2001/222/ln/ BF, ESA-ESTEC, Noordwijk, The Netherlands, 2001.

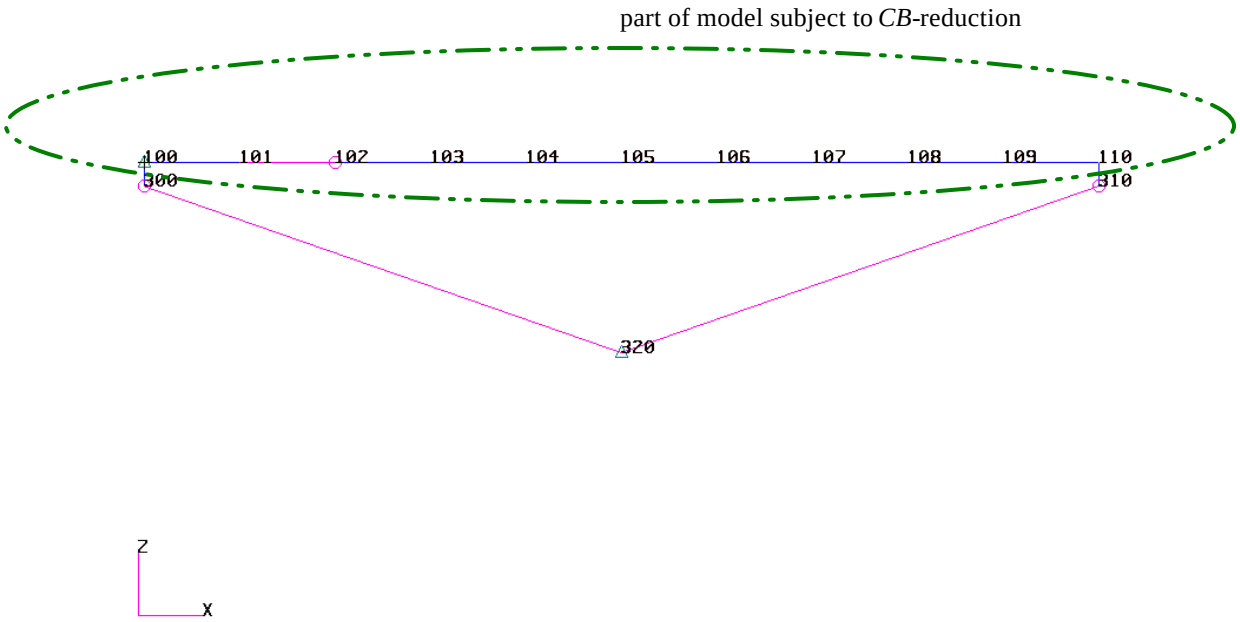

Figure 1: Beam model

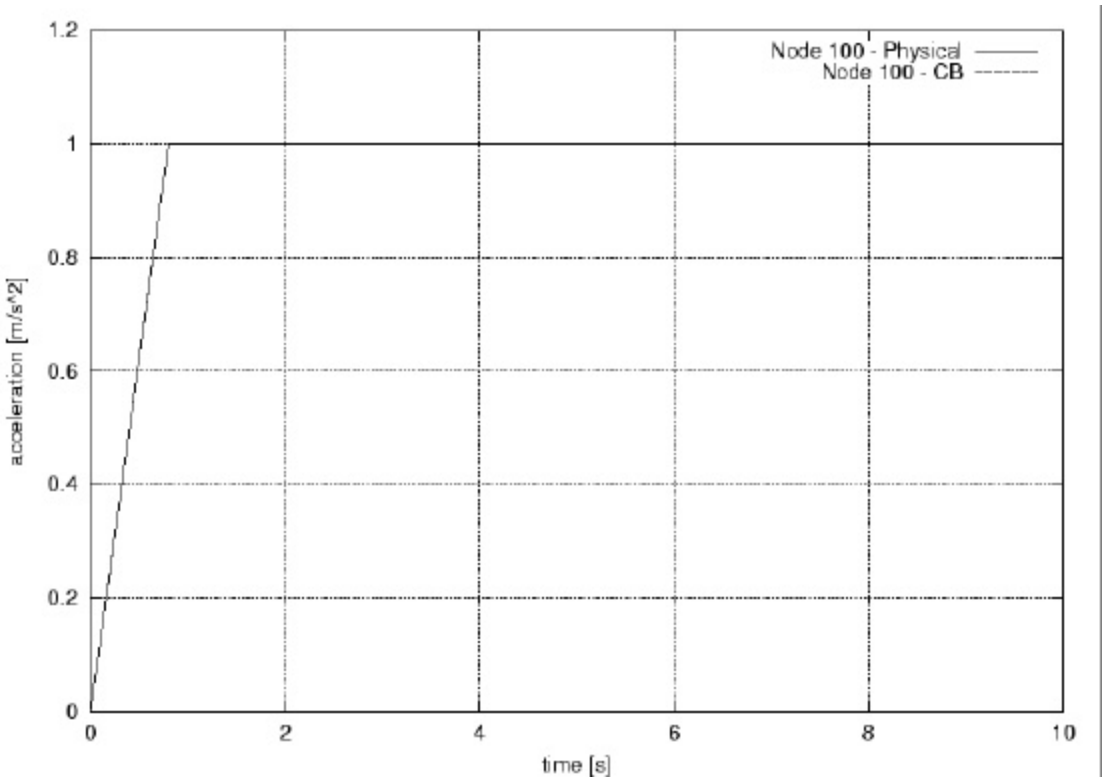

Figure 2: Input acceleration at end-points

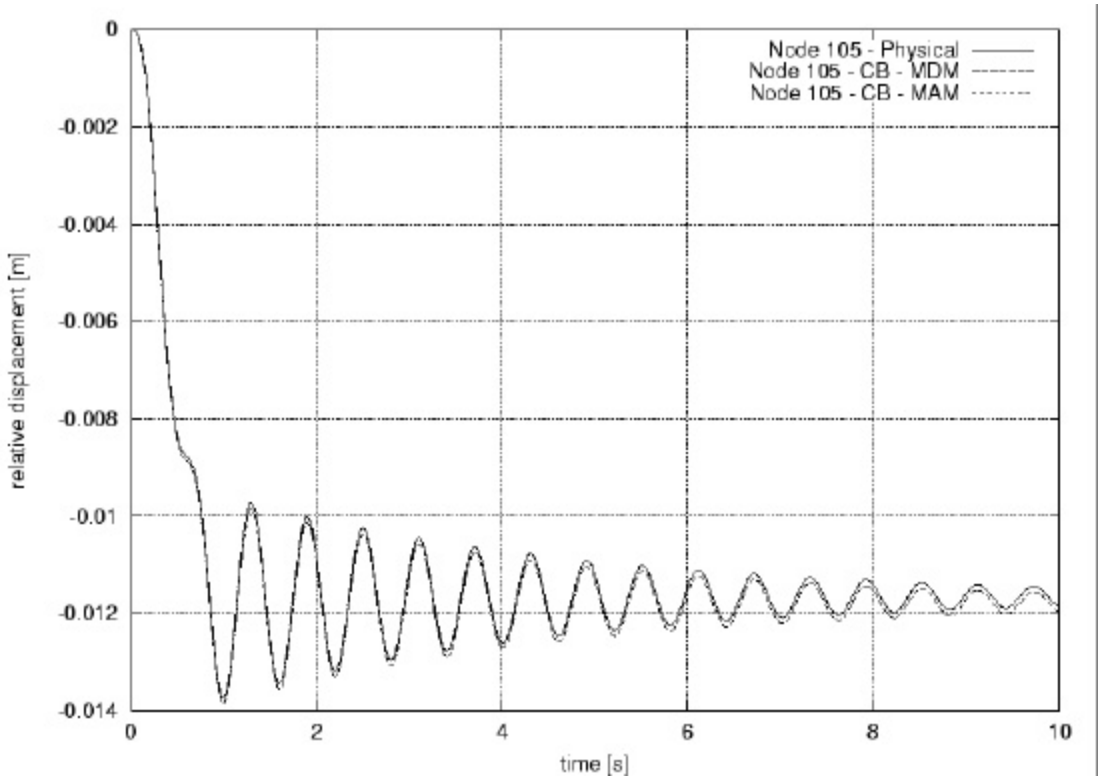

Figure 3: Relative displacement of node 105

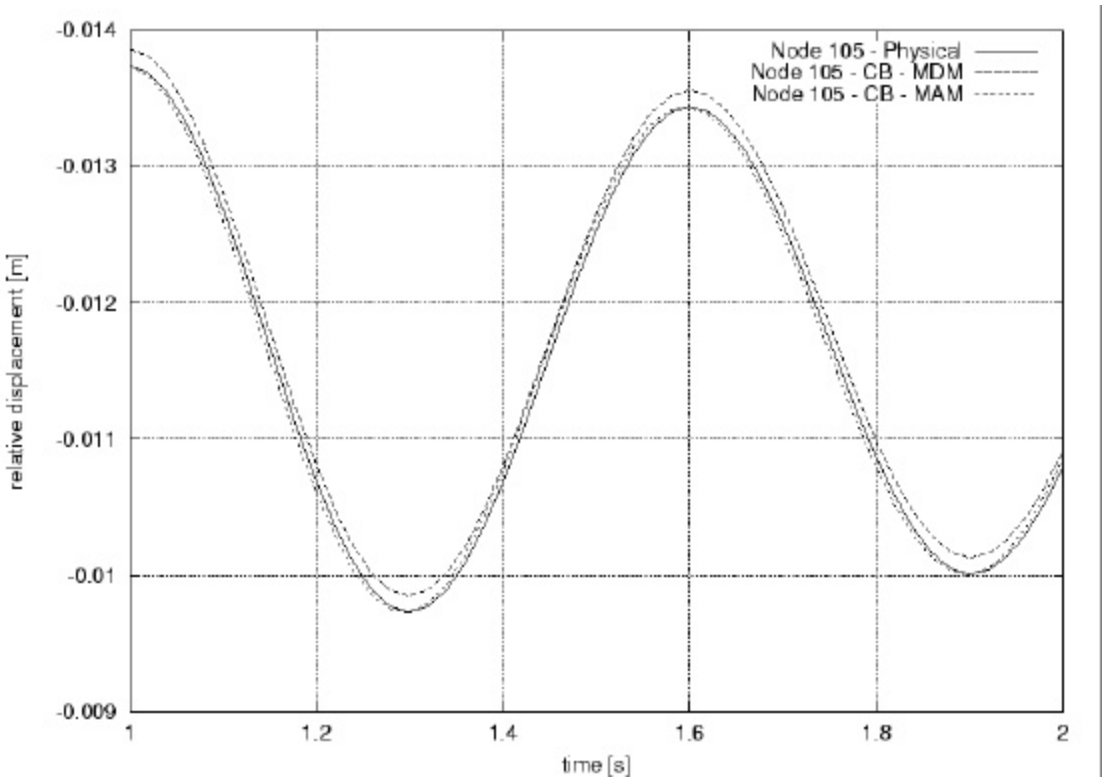

Figure 4: Relative displacement / [1-2]s

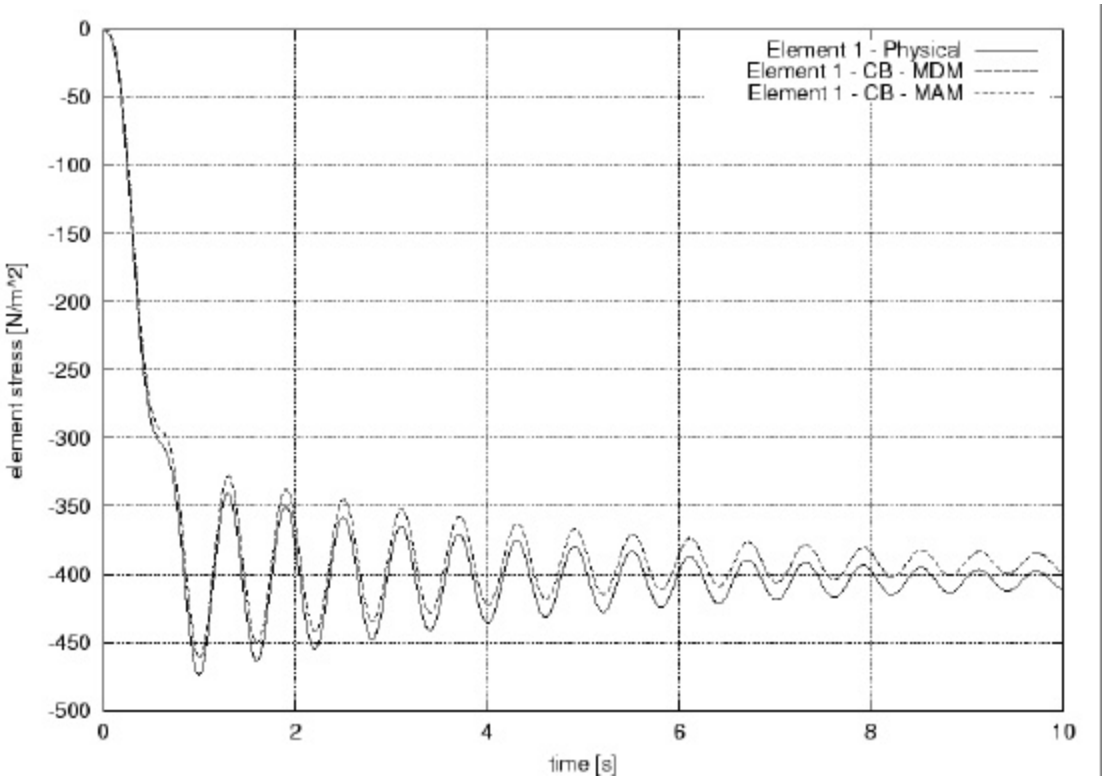

Figure 5: Element stress (CBAR element)

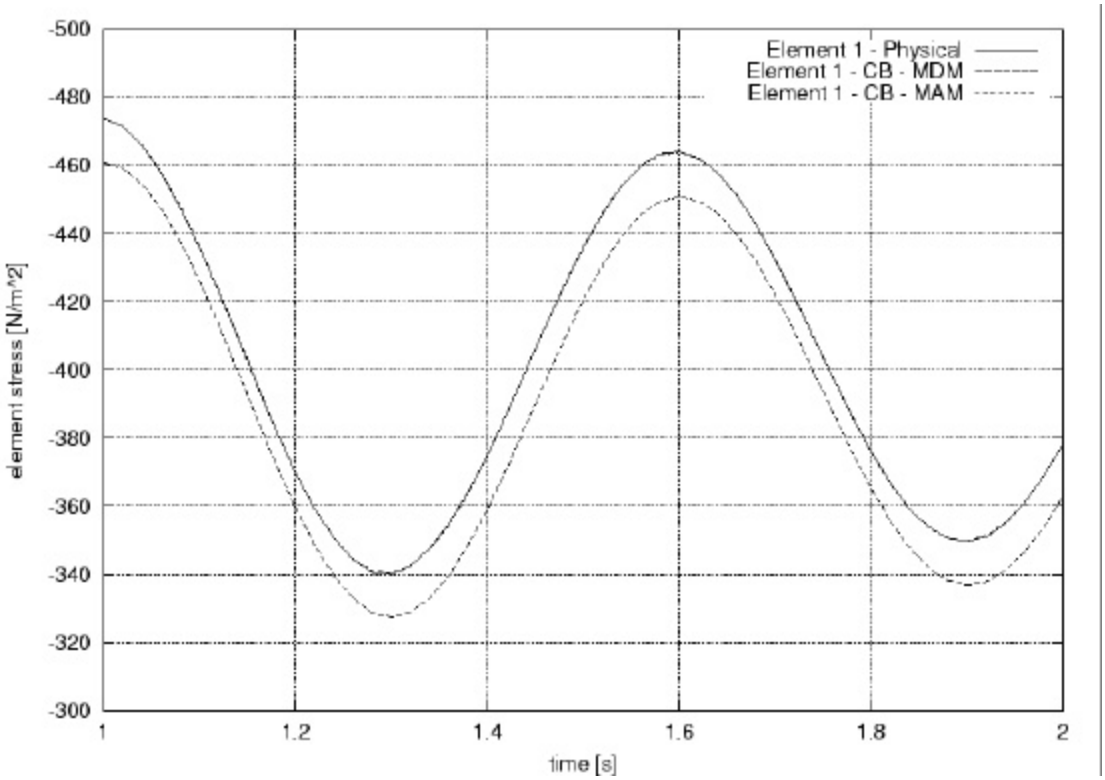

Figure 6: Element stress (CBAR element) / [1-2] s

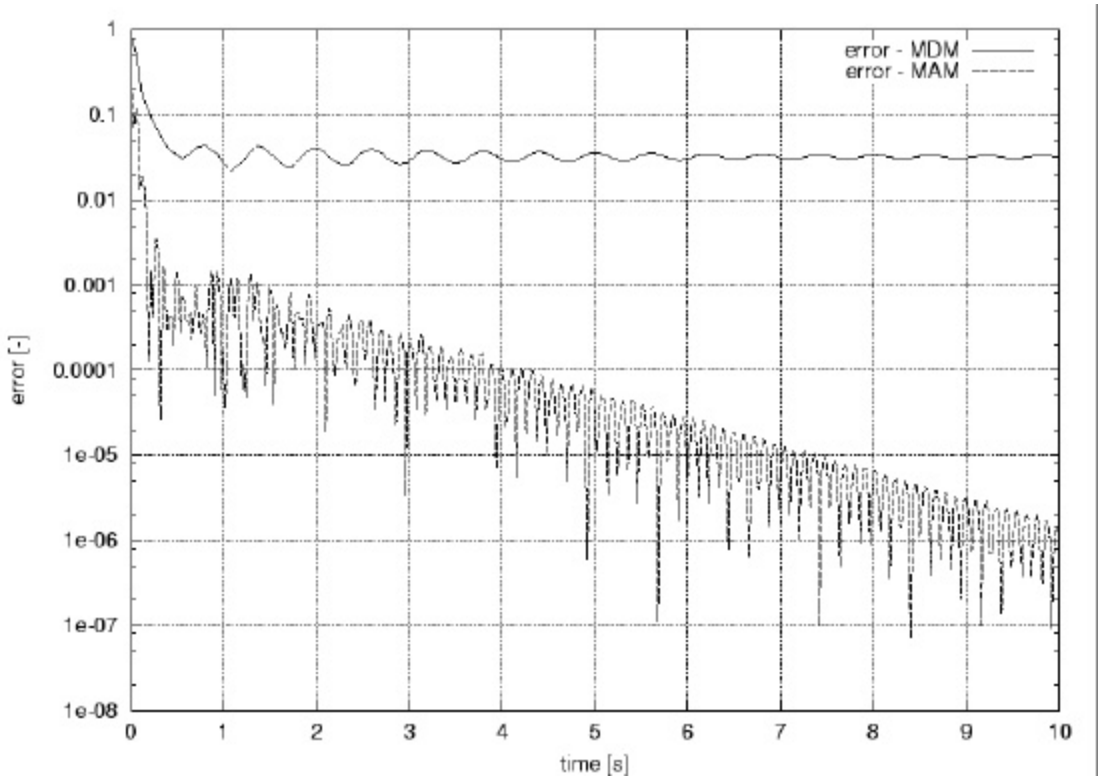

Figure 7: Error in element stress relative to physical solution

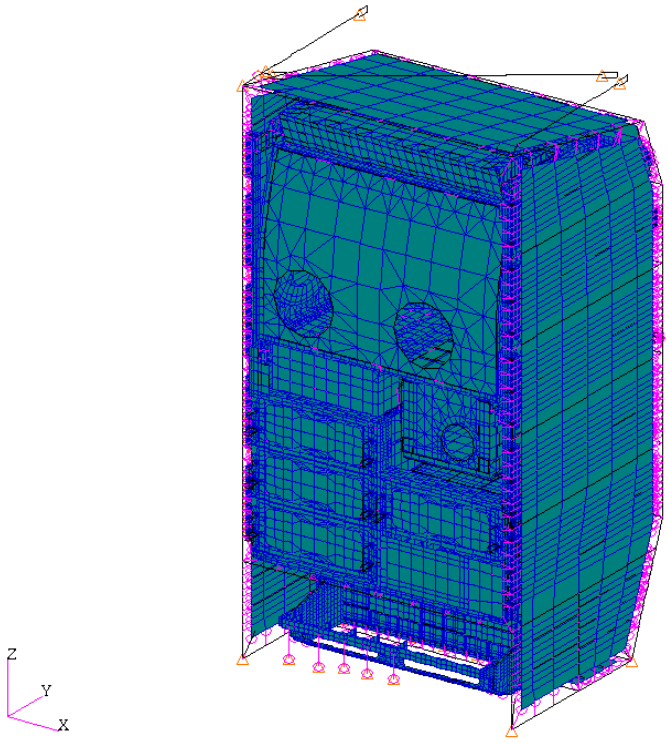

Figure 8: Payload Rack

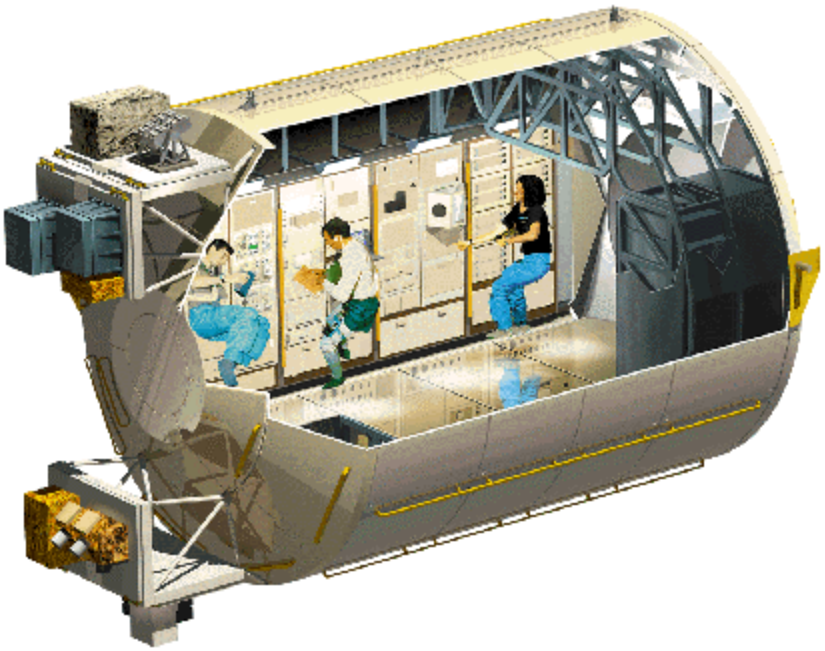

Figure 9: *ESA*'s Columbus Orbital Facility